DETERMINATION OF PARAMETERS AND EPIDEMIOLOGICAL FORECASTING USING MULTI-GENERATIONAL SIR MODELING

Abstract. We use an age-dependent SIR system of equations to model the evolution of the COVID-19, taking different social and biological traits into account. Parameters that measure the amount of interaction in different locations (home, work, school, other) are approximated using a random optimization scheme, and indicate changes in social activities along the course of the pandemic. Taking previously determined parameters, we are able to make predictions for different scenarios. We compare our predictions with data from several locations in Brazil.

1. Introduction

Several months after the onset of the COVID-19 pandemic, it becomes clear how powerful numerical models can be used to predict different scenarios. In particular, compartimental epidemiological models are convenient, depending on few parameters and still capturing with reasonable precision essential aspects of the dynamics of infectious diseases.

The Susceptible-Infected-Recovered *SIR* modeling in its simplest form depends on two parameters, the average number of *adequate contacts* (those sufficient for transmission) and the *mean waiting period* in which the patient is infectious. It assumes that the population is homogeneous both in terms of behavior and biological susceptibility. It also assumes, in its simplest instance, that demographic aspects as age structure, natality and death rates do not matter for the dynamics of the disease.

Some of the above assumptions appear to hold well in the case of the COVID-19 pandemic. Demographic changes appear to be of less importance due to difference in time scales, compared with the evolution of the pandemic. Also, the period that one is infectious seems to be independent of age, to some reasonable extent. However, dropping the homogeneity hypothesis allows a more realistic model because age and location are certainly important in undertanding the dynamics of the disease.

Mathematical epidemiology has a somewhat long history, with Hamer (1906); M'Kendrick (1925); Kermack et al. (1927) being among the earliest contributions. See Brauer (2017); Hethcote (2000) for a thorough review of mathematical modeling of infectious diseases,

Date: November 23, 2020.

Notes by Alexandre Madureira (LNCC, EPGE-FGV), based on joint work with Eduardo Campos (Ence, EPGE-FGV), Rubens Penha Cysne (EPGE-FGV), and Gelcio Mendes (INCA). .

and Klepac and Caswell (2011); Klepac et al. (2009); Iannelli and Milner (2017); Li et al. (2020); Sun (2010); Towers and Feng (2012) for multi-group models. Some other models consider spatial aspects of infectious diseases, as Bertaglia and Pareschi (2020); Lang et al. (2018); Paeng and Lee (2017); Peixoto et al. (2020); Takács and Hadjimichael (2019); Viguerie et al. (2020). Theoretical aspects of models are covered in Kuniya and Wang (2018); Wen et al. (2018); Wu and Zou (2016). For the control related models for COVID-19 see for instance Perkins and España (2020) and references therein.

After the onset of the COVID-19 pandemic, a massive amount of articles related to the topic materialized. Several articles considered compartimental models to forecast different scenarios, as in Atkeson (2020); Prem et al. (2020); Komatsu and Menezes-Filho (2020); Viguerie et al. (2020); Walker et al. (2020).

Socio-economic costs of imposing social distancing are combined with compartimental models in Acemoglu et al. (2020); Alvarez et al. (2020); Atkeson (2020), and the interplay between economics and individual decisions are considered in Borelli and Góes (2020); Brotherhood et al. (2020); Eichenbaum et al. (2020). See Kremer (1996); d'Onofrio and Manfredi (2020); Funk et al. (2015); Manfredi and d'Onofrio (2013); Perrings et al. (2014); Soofi et al. (2020) for a description of behavioral- and economic- epidemiology ideas. Also, macro-economic aspects of the pandemic appears, e.g., in Guerrieri et al. (2020).

Population heterogeneity and its influence on herd immunity is considered in Aguas et al. (2020); Britton et al. (2020); Cui et al. (2019); Gomes et al. (2020). Vaccination is considered in, for instance, d'Onofrio and Manfredi (2020); González and Villena (2020); Jia et al. (2020); May and Anderson (1984).

Finally, alternative approaches, as agent-based and statistical models and a combination of these techniques with compartimental models (specially to gather data), are also commonly employed, as in Bendtsen Cano et al. (2020); Calvetti et al. (2020); Donnat and Holmes (2020); Ferguson et al. (2020); Roda et al. (2020).

In the present paper, we consider a modification of the age-structured SIR model used by Towers and Feng (2012). As in Prem et al. (2017), we allow for age-dependent probabilities of one being sub-clinical or clinical, and use their contact matrices which differentiates not only age but also location. Random searches approximate some key parameters that are related to social distancing in diferent locations, computing their values for some Brazilian regions. Following the approximation of those parameters, we are able to forecast best/worst case scenarios. To gauge the efficiency of the scheme, we compare with available data.

2. The model

In the spirit of compartimental modeling, we divide the whole population among *susceptible* ($\boldsymbol{S}$), *infected* ($\boldsymbol{I}$), *removed* ($\boldsymbol{R}$). Due to the short time scale of the disease, we can assume that demographic changes are not relevant, and deaths are estimated from the removed, $\boldsymbol{R}$. The above quantities are 16-dimensional vectors, stratified by age, running from 0-4 (first components), 5-9 (second components), etc, up to 75-above (16^{th} components). There are P_i individuals for each age group, and the total population $P = \sum_{i=1}^{16} P_i$ is constant.

The equations governing the dynamics of the disease is as follows[1], for $i = 1 \dots, 16$ and $t \in \mathbb{N}$:

$$\begin{aligned} S_i(t+1) &= S_i(t) - \beta_i(\boldsymbol{I})S_i(t), \\ I_i(t+1) &= I_i(t) + \beta_i(\boldsymbol{I})S_i(t) - \gamma I_i(t), \\ R_i(t+1) &= R_i(t) + \gamma I_i(t), \end{aligned} \tag{1}$$

plus initial conditions. The model is "conservative" in the sense that $S_i + I_i + R_i = P_i$ is constant for all ages i.

The term $\beta_i S_i$ is the rate of new infections of the i-population, and we remark that $\boldsymbol{\beta}$ depends on the number of infected of all ages, making the model nonlinear. Those infected are removed from their condition at rate γI_i (they either recover or die). We further divide the infected into two groups, those that are asymptomatic or *sub-clinical* $I_i^{\text{sc}} = (1-\rho_i)I_i$ in the sense that they do not require medical care. The *clinical* group $I_i^{\text{c}} = \rho_i I_i$ corresponds to those that get ill, requiring medical attention. The age-dependent fractions of those who become sub- or clinical are $\rho_i \in [0,1]$.

To fully describe the model, we ought to define $\boldsymbol{\beta}$ and the other parameters.

(i) the components of the incidence function $\boldsymbol{\beta}$ are given by the formula

$$\beta_i(\boldsymbol{I}) = \sum_{j=1}^{16} \frac{\alpha^{\text{sc}} I_j^{\text{sc}} + \alpha^{\text{c}} I_j^{\text{c}}}{P_j} C^e_{i,j} = \sum_{j=1}^{16} \big(\alpha^{\text{sc}}(1-\rho_j) + \alpha^{\text{c}}\rho_j\big)\frac{I_j}{P_j} C^e_{i,j},$$

where C^e is an *effective contact matrix* that measures the number of contacts between age groups. It depends on the *amount* and *choices* of lock-down imposed, as we describe further ahead. The age-independent parameters α^{sc} and α^{c} correspond to the fraction of those infected that have the potential to infect others, due to social behavior or biology. For convenience, we also write the vector $\boldsymbol{\beta}(\boldsymbol{I}) = C^e D\boldsymbol{I}$, where D is a diagonal

[1]Note that we are *not* using the Einstein's summation convention of summing up repeated indices.

matrix defined by

$$D_{jj} = \frac{\alpha^{\mathrm{sc}}(1-\rho_j) + \alpha^{\mathrm{c}}\rho_j}{P_j}.$$

(ii) The time dependent effective contact matrix C^e is defined by

$$C^e(t) = \beta_h(t)C^{\mathrm{home}} + \beta_w(t)C^{\mathrm{work}} + \beta_s(t)C^{\mathrm{school}} + \beta_o(t)C^{\mathrm{other}}, \tag{2}$$

where the exogenous data C^{home}, C^{work}, C^{school}, C^{other} are 16×16 matrices, where C^{ℓ}_{ij} indicates the average number of *different people* from the age group j that someone from the age group i contacted per day at $\ell \in \{\text{home, work, school, other}\}$, as compiled by Mossong et al. (2008); Prem et al. (2017). The parameters β_ℓ control the fraction of contacts that are "adequate", in the sense that they lead to infections.

(iii) Each component of $\boldsymbol{\rho}$ indicates whether an infected individual will become a sub-clinical or a clinical case. Since COVID-19 symptoms are more aggressive for older patients, ρ_i grows with i.

(iv) $\gamma = 1 - e^{-1/d_I}$ indicates the daily probability that someone stays infected, where d_I is the average duration of infection, as in Prem et al. (2017).

(v) The contagious parameters α^{sc} and α^{c} correspond to fractions of sub-clinical and clinical infected patients that still spread the virus.

In Acemoglu et al. (2020), a SIR model that takes into account age is also used, and three groups are considered. The authors include the possibility of using a family of scalings for the incidence function β, but none of them reproduces our own choice.

2.1. **Reproduction and replacement numbers.** The *basic reproduction number* $\mathcal{R}_0$ is understood as *the secondary cases produced by an infected individual introduced in a totally susceptible population*, see Barril et al. (2020); Delamater et al. (2019); Diekmann et al. (1990); Hethcote (2000). Hence, suppose that the whole population with distribution $\boldsymbol{P}$ is susceptible ($\boldsymbol{S} = \boldsymbol{P}$), and we represent the infected individual by $\hat{\boldsymbol{I}}$, a vector belonging to the canonical basis $\{\boldsymbol{e}_1, \ldots, \boldsymbol{e}_{16}\}$. The number of infected individuals in the first day belonging to the i-th is

$$\sum_{k=1}^{16} \delta_{ik}\beta_k(\hat{\boldsymbol{I}})P_k = \sum_{k,j,\ell=1}^{16} \delta_{ik}P_kC_{kj}D_{jl}\hat{\boldsymbol{I}}_l = \sum_{m,j,\ell=1}^{16} \mathbb{P}_{im}C_{mj}D_{jl}\hat{\boldsymbol{I}}_l$$

where δ_{ik} indicates the Kronecker delta, which equals one if $i = j$ and zero otherwise, and we define $\mathbb{P}$ as the diagonal matrix such that $\mathbb{P}_{kk} = P_k$. Let $A = \mathbb{P}CD$. Then the vector containing the contamineted individuals in the first day is $A\hat{\boldsymbol{I}}$, and we can bound its Euclidian

norm as

$$\|A\hat{\boldsymbol{I}}\|_2 \leq \lambda_{\max}\|\hat{\boldsymbol{I}}\|_2 = \lambda_{\max}, \tag{3}$$

where $\lambda_{\max}$ is the largest eigenvalue of A. Note that only the fraction $(1-\gamma)^{d-1}\hat{\boldsymbol{I}}$ of the infected outsider remains infected on the d-th day. Those individuals infect less than $(1-\gamma)^{d-1}\lambda_{\max}$, as in (3), and adding up all days, we gather that the total number of infected agents is bounded by the basic reproduction number

$$\mathcal{R}_0 := \sum_{d=1}^{\infty}(1-\gamma)^{d-1}\lambda_{\max} = \frac{1}{\gamma}\lambda_{\max}. \tag{4}$$

Reasoning in a similar fashion, we define the *replacement number*

$$\mathcal{R}_t := \frac{1}{\gamma}\lambda_{\max}(t), \tag{5}$$

where $\lambda_{\max}(t)$ is defined as the maximum eigenvalue of the matrix $\mathbb{S}CD$ and $\mathbb{S}$ is the diagonal matrix with the diagonal given by S_j for $j = 1, \ldots, 16$.

The above definitions of $\mathcal{R}_0$ and $\mathcal{R}_t$ rely on the Euclidian and spectral norms. However, if one is interested in considering age-dependent quarantine or vaccination policies, it might be interesting to consider the *infinity* norm. In this case, note that the total number of infected individuals on the first day is

$$\boldsymbol{\beta}(\hat{\boldsymbol{I}}) \cdot \boldsymbol{P} = C^e D\hat{\boldsymbol{I}} \cdot \boldsymbol{P} = \sum_{i,j=1}^{16} C^e_{ij} D_{jj} I_j P_i \leq \|\boldsymbol{P}^T CD\|_\infty, \tag{6}$$

where $\|\boldsymbol{v}\|_\infty = \max\{|v_i| : i = 1, \ldots, 16\}$ for a vector $\boldsymbol{v}$ of size 16. The above estimate holds since all quantities involved are non-negative. We remark that the estimate is sharp since, for at least one vector of the canonical basis, the inequality (6) becomes an identity. As before, adding up the days and considering that at the jth day there will be a fraction $(1-\gamma)^{d-1}\hat{\boldsymbol{I}}$ of infected outsider, we gather that the total number of infected agents is bounded by

$$\mathcal{R}_{0,\infty} := \sum_{d=1}^{\infty}(1-\gamma)^{d-1}\|\boldsymbol{P}^T CD\|_\infty = \frac{1}{\gamma}\max\left\{\frac{(\alpha^{\mathrm{sc}}(1-\rho_j)+\alpha^{\mathrm{c}}\rho_j)}{P_j}\sum_{i=1}^{16} C^e_{ij}P_i : 1 \leq j \leq 16\right\}. \tag{7}$$

Similarly, we define the corresponding replacement number

$$\mathcal{R}_{t,\infty} := \frac{1}{\gamma}\max\left\{\frac{(\alpha^{\mathrm{sc}}(1-\rho_j)+\alpha^{\mathrm{c}}\rho_j)}{P_j}\sum_{i=1}^{16} C^e_{ij}S_i : 1 \leq j \leq 16\right\}. \tag{8}$$

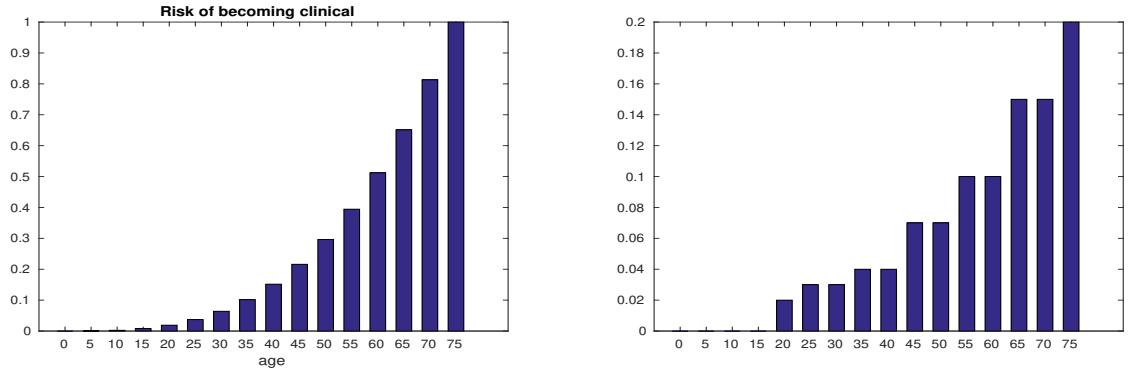

FIGURE 1. Probability of being clinical among infected patients $\boldsymbol{\rho}$ (left) and lethality weight $\boldsymbol{w}_d$ (right).

2.2. **Modeling the lethality.** Mortality is not part of the dynamics[2], resulting from the number of infected patients. We postulate that only those clinically infected die, at an age-dependent rate. So, among the "recovered" patients, $d(t) = \gamma\mu(t)\boldsymbol{w}_d \cdot \boldsymbol{I}^{\mathrm{c}}(t)$ die, where $\boldsymbol{w}_d$ is the lethality weight of the disease and the *letality strength* μ captures how letality varies with time. We assume that age-related lethality might vary across different regions and with time, but *the proportion* between different ages is constant.

2.3. **Data.** The transmission parameters α^{sc} and α^{c} are such that the transmission rate of asymptomatic is 60% larger than those symptomatic. This ad hoc choice is based on the assumption that symptomatic patients are more likely to quarantine themselves.

We stipulate that the proportion of symptomatic patients are as in Figure 1 (left), assuming that the proportion of symptomatic patients follows the same pattern of the infected that were hospitalized, as reported in Verity et al. (2020). However, the proportion of asymptomatic infected patients is far from being settled, with estimates ranging from 5% to 80%, as described in Heneghan et al. (2020).

Similarly, we assume that the lethality rates are as Figure 1 (right), and we assume that the proportions follow Brazeau et al. (2020); Verity et al. (2020).

The contact matrices C^{home}, C^{work}, C^{school}, C^{other} are from Prem et al. (2017), and population data, as seen in Figure 2 is from the Instituto Brasilerio de Geografia e Estatística (IBGE). The average number of days d_I that a patient is infectious is set to 12.

We use the available data (number of new cases and deaths) from each location to estimate the remaining functions $\beta_h(t)$, $\beta_w(t)$, $\beta_s(t)$, $\beta_o(t)$ used to define the effective matrix C^e in (2), and $\mu(t)$ defined in Section 2.2. These functions are transient since not only individuals

[2]We assume that the recovered patients do not get reinfected.

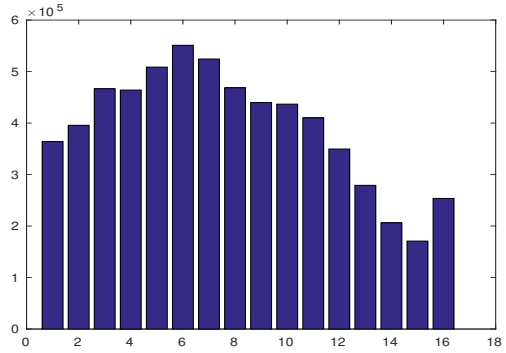

FIGURE 2. Population of the city of Rio de Janeiro.

change behavior with time, as in Brotherhood et al. (2020), but also lethality rates decay as the medical expertise increases with time.

For a simple SIR model, the available data uniquely determines the parameters, as in Bakhta et al. (2020). In general, that is not the case for our model, for instance if one of the four contact matrices vanish or if $C^{\text{work}} = C^{\text{other}}$. We make then some simplifying hypotheses. First, we assume that β_h is constant, as there is no reason to expect that the amount of contacts at home varies significantly with time. The second assumption is that $\beta_s(t)$ is identically zero, since schools were closed during the period of data gathering. We also suppose that $\beta_w = \beta_o$, i.e., the behaviour at work is equal to the behavior at other locations. Such assumption aims to reduce possible indeterminations of the parameters.

Consider that data is available for the period $\{1, \dots, T\} \subseteq \mathbb{N}$, and let and $\mathcal{N}_{\mathcal{I}}^{\text{data}}(j)$ and $\mathcal{N}_{\mathcal{D}}^{\text{data}}(j)$ be the number of new cases and new deaths at the j-th day. For simplicity, assume that $T = N\delta t$ where $\delta t = 10$, and consider the partition $\mathcal{T}_{\delta t}$ of $\{1, \dots, T\} = \cup_{j=1}^{N} I_j$ where

$$\mathcal{T}_{\delta t} = \big\{ I_j : j = 1, \dots, N \big\}, \qquad I_j = \big\{ (j-1)\delta t + 1, j\delta t \big\}.$$

Let $P_0(\mathcal{T}_{\delta t})$ be the space of piecewise constant functions with respect to the above partition. To determine β_w we pose the problem of finding (β_h, β_w) that solves

$$\min_{(\hat{\beta}_h, \hat{\beta}_w) \in \mathbb{R} \times P_0(\mathcal{T}_{\delta t})} J(\hat{\beta}_h, \hat{\beta}_w), \qquad \text{where} \qquad J(\hat{\beta}_h, \hat{\beta}_w) = \frac{\|\mathcal{N}_{\mathcal{I}}^{\text{sir}}(\hat{\beta}_h, \hat{\beta}_w) - \mathcal{N}_{\mathcal{I}}^{\text{data}}\|_{\mathbb{R}^T}}{\|\mathcal{N}_{\mathcal{I}}^{\text{data}}\|_{\mathbb{R}^T}}, \tag{9}$$

and $\|\cdot\|_{\mathbb{R}^T}$ is the Euclidian norm in $\mathbb{R}^T$. Above, $\mathcal{N}_{\mathcal{I}}^{\text{sir}}(\hat{\beta}_h, \hat{\beta}_w)(t)$ is the number of new infected clinical patients that the SIR model (1) yields at the t-th day if one replaces β_h and β_w by $\hat{\beta}_h$ and $\hat{\beta}_w$ in (2).

The above problem has finite dimension $N+1$ since any function $\beta \in P_0(\mathcal{T}_{\delta t})$ can be written as

$$\beta_w(t) = \sum_{j=1}^{N} b_j \chi_{I_j}(t) \tag{10}$$

for some unknown coefficients $b_1, \ldots, b_N \in \mathbb{R}$, where $\chi_{I_j}(t)$ is the characteristic function of I_j, which equals one if $t \in I_j$, and zero otherwise. The coefficients uniquely define a function in $P_0(\mathcal{T}_{\delta t})$ and vice-versa.

To solve (9) we employ a random optimization approach

(i) Choose a initial guess (β_h, β_w)
(ii) While some convergence criteria is not reached
  (a) Define $(\hat{\beta}_h, \hat{\beta}_w)$ from (β_h, β_w) by adding noise
  (b) If $J(\hat{\beta}_h, \hat{\beta}_w) < J(\beta_h, \beta_w)$, then $(\beta_h, \beta_w) \leftarrow (\hat{\beta}_h, \hat{\beta}_w)$

The estimation of the letality strength μ is based on the number of daily deaths data $\mathcal{N}_{\mathcal{D}}^{\text{data}}$. The total number of deaths simulated by the SIR model is given by $\gamma\mu(t)\boldsymbol{w}_d \cdot \boldsymbol{I}^{\text{c}}(t)$. Equating both quantities we compute

$$\mu(t) = \frac{\mathcal{N}_{\mathcal{D}}^{\text{data}}(t)}{\gamma \boldsymbol{w}_d \cdot \boldsymbol{I}^{\text{c}}(t)}. \tag{11}$$

3. Simulation of the dynamics of the disease

In what follows we show the results coming out of parameter estimations. We then show results adressing how well the model predicts the number of new cases. We compare with real daily data for new cases and deaths[3]. To smooth out oscillations, we present the data using a 7-day moving average.

One of the hurdles for models as ours is the definition of initial conditions, since when the virus started to spread and how many were the first infected individuals are not known. As a initial condition of our model, we assume that the first infected case occurred 30 days before the official recordings. Indeed, the first day of the official data logs 489 cases, and the real initial condition of the system is not known; cf. Lourenço et al. (2020), who speculates that the epidemic in Italy and UK started one month before the first reported death. We also estipulate that there were 10 infected patients at each age group at day one.

[3]All data were from taken from `https://covid.saude.gov.br/`, an official site from the Brazilian's Government Department of Health.

Such uncertainty of initial conditions makes the results unreliable at the initial periods of simulations. In particular, the computation of (11) is not feasible for the lack of data. We make then $\mu(j) = 1$ at the initial stages.

3.1. **Parameter estimations, and prediction analysis.** We consider results for the City of Rio de Janeiro, first presenting the computed results for all variables, adding up the values for all ages, i.e.

$$S(t) = \sum_{j=1}^{16} S_j(t), \qquad I^{\mathrm{sc}}(t) = \sum_{j=1}^{16} I_j^{\mathrm{sc}}(t), \qquad I^{\mathrm{c}}(t) = \sum_{j=1}^{16} I_j^{\mathrm{c}}(t), \qquad R(t) = \sum_{j=1}^{16} R_j(t).$$

We recall the assumption that the contacts might lead to infections at home are time independent, and the contacts at work and other locations have a similar pattern, i.e., $\beta_w = \beta_o$. Also, schools are closed, thus $\beta_s = 0$.

We display in Figure 3 the results of our parameter estimations; see the caption for a detailed description of each individual plot. We note that the results from the model are accurate, approximating well the data and capturing the dynamics of the desease. In particular we see that β_w (top-right plot) oscillates following the "macroscopic" oscillations of daily cases (top-left plot). Regarding the letality, we note the decrease of its strength after day 90, in line with what was presented by Dennis et al. (2020); Horwitz et al. (2020).

Two important pieces of information that comes out of the modeling are the value of the reproduction and replacement numbers $\mathcal{R}_0$ and $\mathcal{R}_t$, and these computations follow easily from (4) and (5). We display the results in Figure 4 (left figure). Note that values of $\mathcal{R}_0$ is characterized only by the β's and the data, while $\mathcal{R}_0$ depends also on the dynamics of the disease through the susceptible population. That is important since even if $\mathcal{R}_0 > 1$, having $\mathcal{R}_t$ smaller than one is enough to have a declining number of infected patients.

Another issue that is worth discussing is that we fit the number of clinically infected patients I^{c} to the data. However, we discussed nothing thus far about the sub-clinical patients I^{sc}. It turns out that the number of subclinical patients is, in this case, roughly ten times the number of registred patients, as shown in Figure 4 (right figure). Such difference ressonates with often claims that there is a significant sub-notification. For instance, Havers et al. (2020) reports that the number of cases in the US might be at least 10 times of what is registered. It would not come as a surprise if this difference is even greater in Rio. Also, the WHO states that 80% of infections are mild or asymptomatic[4], in particular among children,

[4]https://www.who.int/emergencies/diseases/novel-coronavirus-2019/question-and-answers-hub/q-a-detail/q-a-similarities-and-differences-covid-19-and-influenza

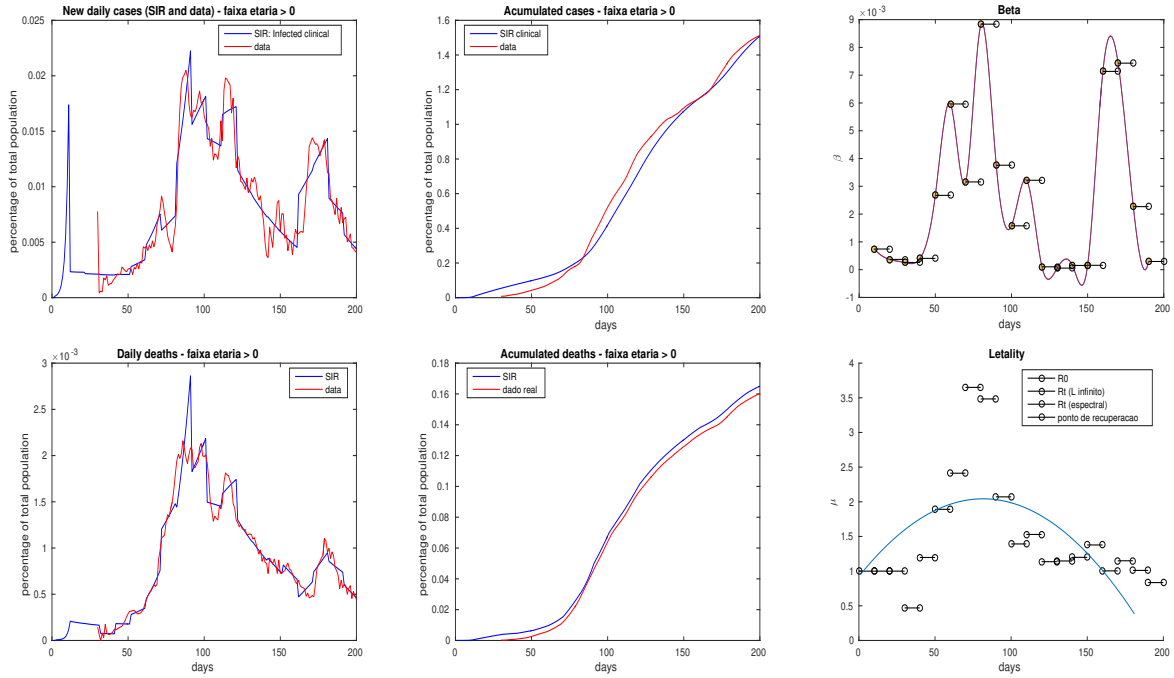

FIGURE 3. Results for the City of Rio de Janeiro. On the first couple of figures on the top we plot the new cases for each day, and the accumulated results. The red plot corresponds to real data, and the black plot depicts clinical cases modeled by SIR. On the top right we plot the estimated values of β_w, except for the first (that has a value roughly ten times bigger than the others). For visualization pourposes we interpolated the discontinuous function β_w using cubic splines. The figures on the bottom are related to fatalities. The first and the second figures show daily and accumulated cases. The third figure displays the values of the letality strength μ, defined in (11). The blue curve is the least square quadratic curve.

as discussed by DeBiasi and Delaney (2020); Han et al. (2020). Recall that children are often not tested.

Next we investigate numerically if this model can make reasonable predictions. To do so, after the day 200, we run the simulations with frozen values of β_w and μ and compare with available data. We perform experiments considering the best and worst scenarios, i.e. lowest and highest number of cases and deaths. We do so by going back j 10-day periods and performing simulations with the highest and lowest values of β_w and μ in the period $200 - 10j$ and 200.

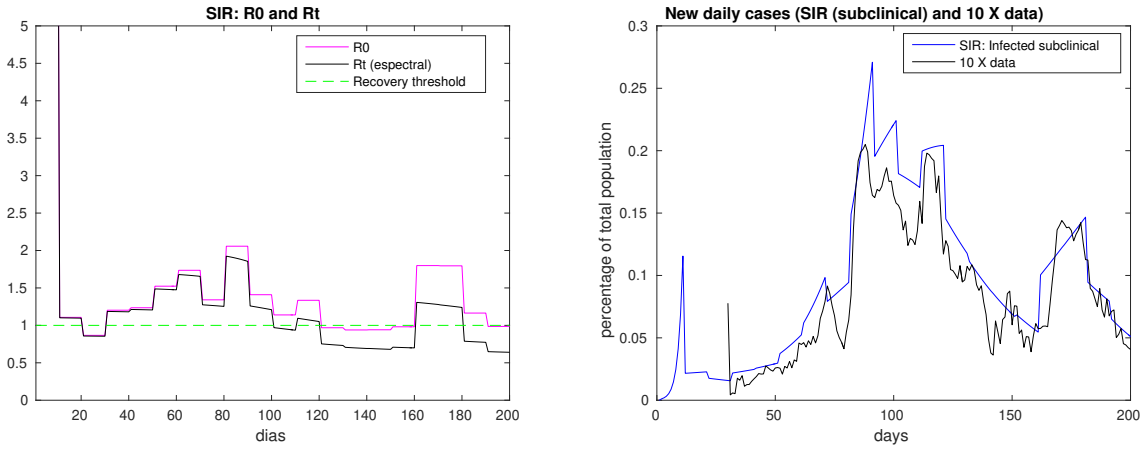

FIGURE 4. Reproduction and replacement numbers (left) and subclinical cases (right) for the city of Rio de Janeiro for the City of Rio de Janeiro.

Choosing $j = 4$, we show in Figure 5 the predicted number of new daily and acumulated cases and deaths with 50 days in advance. Note that, for most of the period of interest, the data is contained between the maximum and minimum value of predicted cases. We also plot results corresponding to the choice of β_w and μ being the average of the extreme values, yielding a more accurate prediction.

Regarding predictions for a long-term future (200 days), we plot in Figure 6 the acumulate cases for best, worst and average scenarios. We remark that the long term predictions in terms of number of deaths are pessimistic, since letality it is very likely that letality will continue to decrease in the future. And, of course, we do not consider the arrival of vaccines in our model.

3.2. **Other locations.** We next perform the same parameter estimation and prediction analysis for different regions. We show the respective results for the city of Petrópolis (Figure 7), State of Rio de Janeiro (Figure 8), City of São Paulo (Figure 9), State of São Paulo (Figure 10) and Brazil (Figure 11). Excepting for the number of cases for the whole country, the estimates are accurate enough. We remark that for Brazil's case, the prediction are for 83 days in advance since more data is available.

4. Discussions and conclusion

Epidemics as the COVID-19 are hard to model, not only because of biological factors, but also due to the unpredicability of human responses. Political, economical, social and individual factors influence the behavior of people, leading to various degrees of risk behavior.

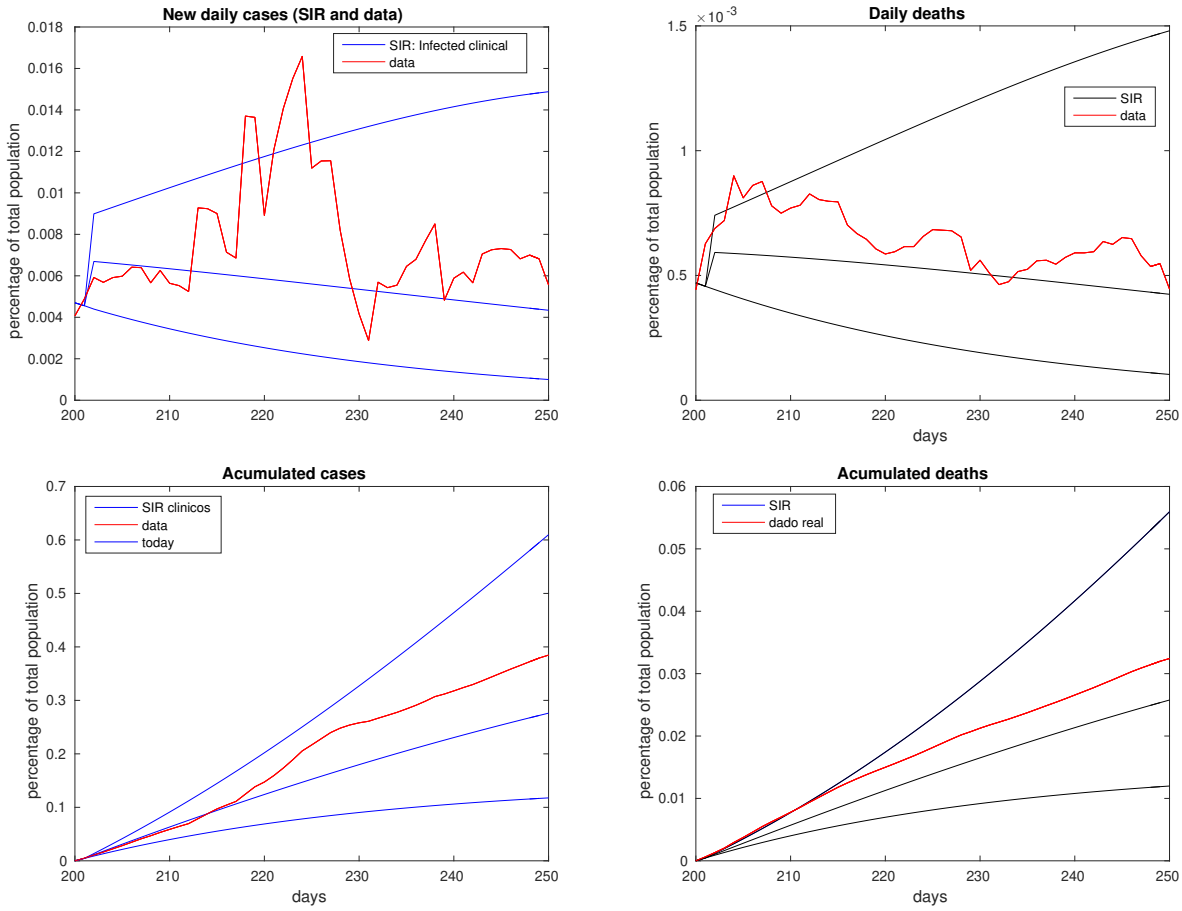

FIGURE 5. The top figures display the number of daily new cases and deaths, while the ones on the bottom display cumulative results. In all cases, the red plots indicates the data and blue represents the simulation results for frozen β_w and μ correspoding to the best and worst case scenarios.

Making long term predictions is riskier than usual in biological systems, but they are crucial for planning non-pharmaceutical interventions, allocation of resources, economical decisions, etc.

What we propose in the work is a general form to predict possible values of crucial parameters based on their past values. The main idea shares similarities with some Value at Risk analyses used in risk management, where the past dynamics of investiments help in predicting the future.

Our method has two steps. Basing the dynamics of the disease on a multi-generational SIR model, we first determine the values of some time-dependent parameters, using a random optimization algorithm. Then, we feed the SIR model using extreme values of such

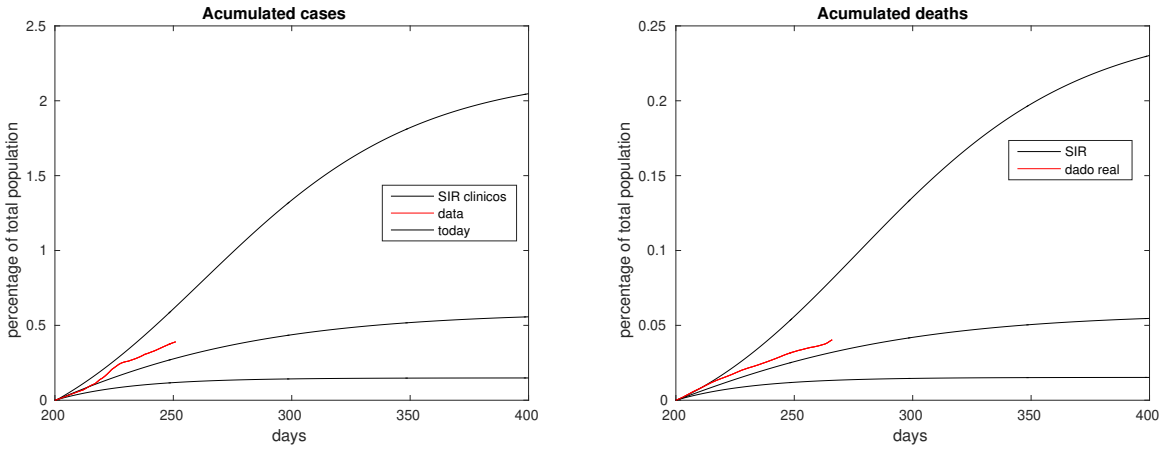

FIGURE 6. Long term predictions for accumulated cases (left) and deaths (right) in the City of Rio de Janeiro. As before, the data is on red, and the SIR model results are in black. In both figures, the top/bottom graphs display the worst/best case scenario. The middle graph diaplsys the results when we take the average of the best/worst parameters.

parameters, and predict best/worst case scenarios. We are also consider a prediction that is between the two extreme cases.

We tested the method for two different states (Rio de Janeiro and São Paulo), and their capitals, predicting the dynamics for 50 days. In all tests, the method performed well, and the accumulated cases and deaths stayed within or very close to the bounds. We also tested for the whole Brazilian country for 83 days, getting good results for the accumulated deaths. For the accumulated cases, the results are not so good. That might be due to the extended period of prediction, or simply because the SIR model might not be appropriate for a large contry like Brazil.

Altough we did not exploit this possibility, the SIR model used by us allows the investigation of "what-if" scenarios. For instance, what would happen if we open schools? Or what if we isolate the elderly population? What if we vaccinate the population of a predetermined age?

The methodology is general and can be applied to other systems and circunstances, and might be usefull to make long-term predictions in situations where unexpected occurances might change the behavior of the system.

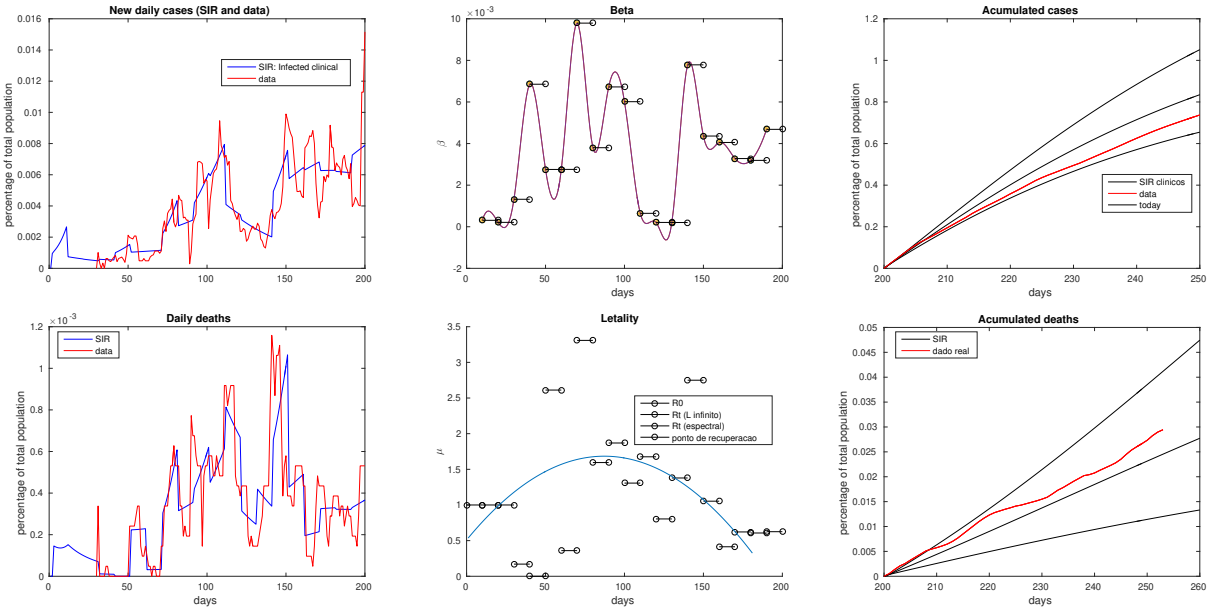

FIGURE 7. City of Petrópolis. Top left: new daily cases computed by SIR (blue) and data (red). Top middle: values of β_w. Top right: predictions for acumulated number of new cases; Bottom left: daily deaths computed by SIR (blue) and data (red). Bottom middle: μ (black) and blue curve is the least square quadratic parabola (blue). Bottom right: predictions for acumulated total deaths.

REFERENCES

Daron Acemoglu, Victor Chernozhukov, Iván Werning, and Michael D Whinston. A multi-risk sir model with optimally targeted lockdown. Working Paper 27102, National Bureau of Economic Research, May 2020. URL `http://www.nber.org/papers/w27102`.

Ricardo Aguas, Rodrigo M. Corder, Jessica G. King, Guilherme Goncalves, Marcelo U. Ferreira, and M. Gabriela M. Gomes. Herd immunity thresholds for sars-cov-2 estimated from unfolding epidemics. *medRxiv*, 2020. doi: 10.1101/2020.07.23.20160762. URL `https://www.medrxiv.org/content/early/2020/07/24/2020.07.23.20160762`.

Fernando E Alvarez, David Argente, and Francesco Lippi. A simple planning problem for covid-19 lockdown. Working Paper 26981, National Bureau of Economic Research, April 2020. URL `http://www.nber.org/papers/w26981`.

Andrew Atkeson. What will be the economic impact of COVID-19 in the US? Rough estimates of disease scenarios. Working Paper 26867, National Bureau of Economic Research, March 2020. URL `http://www.nber.org/papers/w26867`.

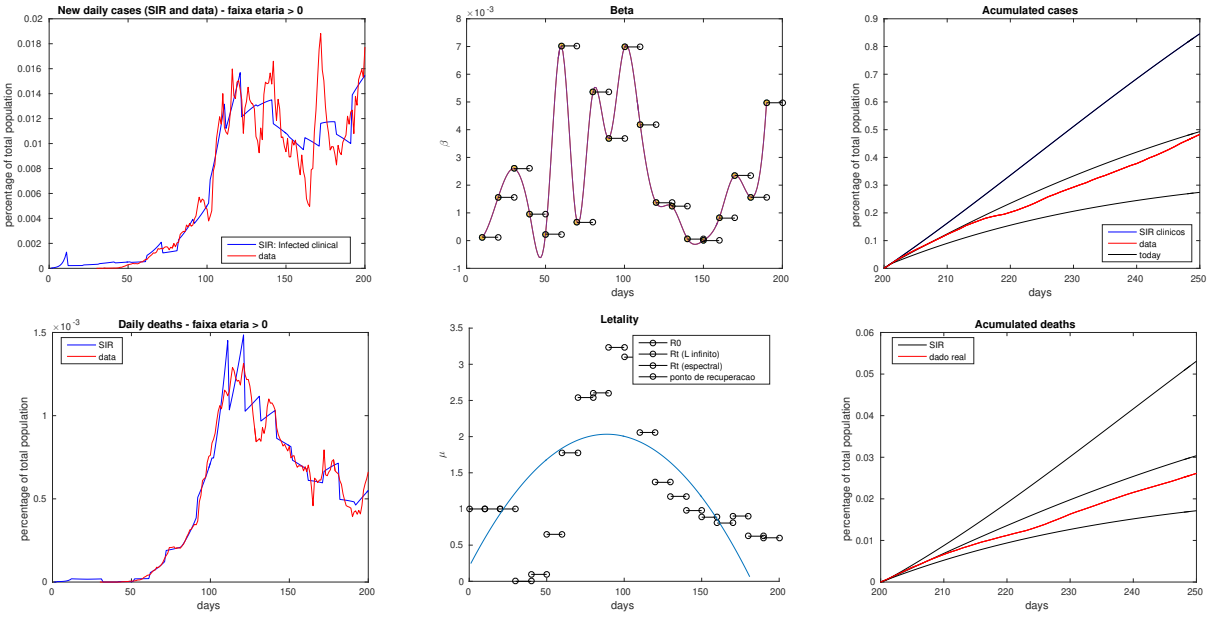

FIGURE 8. State of Rio de Janeiro. Top left: new daily cases computed by SIR (blue) and data (red). Top middle: values of β_w. Top right: predictions for acumulated number of new cases; Bottom left: daily deaths computed by SIR (blue) and data (red). Bottom middle: μ (black) and blue curve is the least square quadratic parabola (blue). Bottom right: predictions for acumulated total deaths.

Athmane Bakhta, Thomas Boiveau, Yvon Maday, and Olga Mula. Epidemiological short-term forecasting with model reduction of parametric compartmental models. application to the first pandemic wave of covid-19 in france, 2020.

Carles Barril, Ángel Calsina, Sílvia Cuadrado, and Jordi Ripoll. On the basic reproduction number in continuously structured populations. *Mathematical Methods in the Applied Sciences*, n/a(n/a), 2020. doi: 10.1002/mma.6787. URL `https://onlinelibrary.wiley.com/doi/abs/10.1002/mma.6787`.

Oliva Bendtsen Cano, Sabrina Cano Morales, and Claus Bendtsen. COVID-19 modelling: the effects of social distancing. *medRxiv*, 2020. doi: 10.1101/2020.03.29.20046870. URL `https://www.medrxiv.org/content/early/2020/03/30/2020.03.29.20046870`.

Giulia Bertaglia and Lorenzo Pareschi. Hyperbolic models for the spread of epidemics on networks: kinetic description and numerical methods, 2020.

Luan Borelli and Geraldo Sandoval Góes. A macroeconomia das epidemias: heterogeneidade interestadual no brasil. Preprint IPEA, 2020.

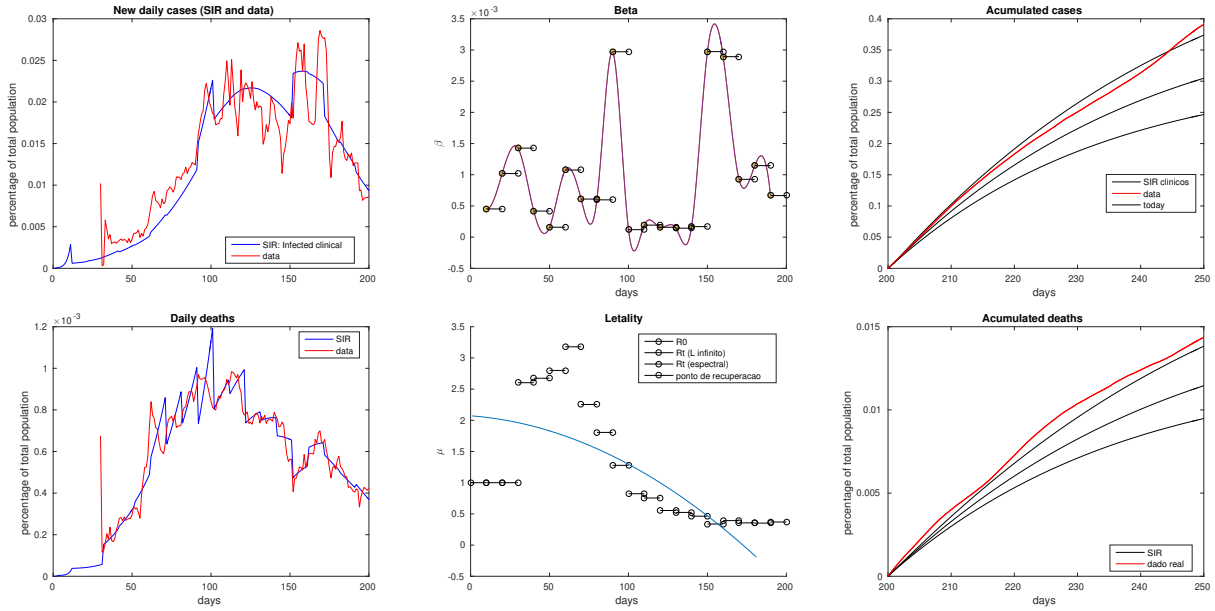

FIGURE 9. City of São Paulo. Top left: new daily cases computed by SIR (blue) and data (red). Top middle: values of β_w. Top right: predictions for acumulated number of new cases; Bottom left: daily deaths computed by SIR (blue) and data (red). Bottom middle: μ (black) and blue curve is the least square quadratic parabola (blue). Bottom right: predictions for acumulated total deaths.

Fred Brauer. Mathematical epidemiology: Past, present, and future. *Infectious Disease Modelling*, 2(2):113 – 127, 2017. ISSN 2468-0427. doi: https://doi.org/10.1016/j.idm.2017.02.001. URL `http://www.sciencedirect.com/science/article/pii/S2468042716300367`.

Nicholas F Brazeau, Robert Verity, Sara Jenks, Han Fu, Charles Whittaker, Peter Winskill, Ilaria Dorigatti, Patrick Walker, Steven Rileyand Ricardo P Schnekenbergand Henrique Hoeltgebaum, Thomas A Mellan, Swapnil Mishra, H Juliette T Unwin, Oliver J Watson, Zulma M Cucunubá, Marc Baguelin, Lilith Whittles, Samir Bhatt, Azra C Ghani, Neil M Ferguson, and Lucy C Okell. Covid-19 infection fatality ratio: Estimates from seroprevalence. resreport 34, Imperial College, October 2020. URL `https://www.imperial.ac.uk/mrc-global-infectious-disease-analysis/covid-19/report-34-ifr/`.

Tom Britton, Frank Ball, and Pieter Trapman. A mathematical model reveals the influence of population heterogeneity on herd immunity to sars-cov-2. *Science*, 2020. ISSN 0036-8075. doi: 10.1126/science.abc6810. URL `https://science.sciencemag.org/content/`

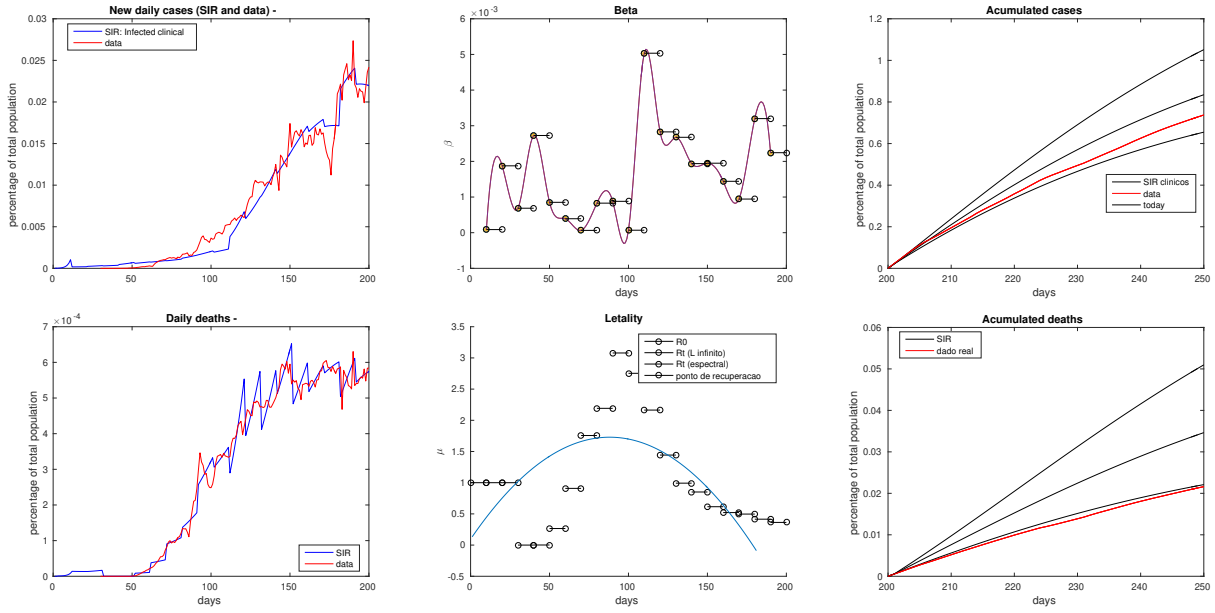

FIGURE 10. State of São Paulo. Top left: new daily cases computed by SIR (blue) and data (red). Top middle: values of β_w. Top right: predictions for acumulated number of new cases; Bottom left: daily deaths computed by SIR (blue) and data (red). Bottom middle: μ (black) and blue curve is the least square quadratic parabola (blue). Bottom right: predictions for acumulated total deaths.

early/2020/06/22/science.abc6810.

Luiz Brotherhood, Philipp Kircher, Cezar Santos, and Michèle Tertilt. An economic model of the covid-19 epidemic: The importance of testing and age-specific policies. resreport 13265, IZA Institute of Labor Economics, May 2020. URL https://www.iza.org/publications/dp/13265.

Daniela Calvetti, Alexander Hoover, Johnie Rose, and Erkki Somersalo. Bayesian dynamical estimation of the parameters of an se(a)ir covid-19 spread model, 2020.

Jingan Cui, Yanan Zhang, and Zhilan Feng. Influence of non-homogeneous mixing on final epidemic size in a meta-population model. *Journal of Biological Dynamics*, 13(sup1):31–46, 2019. doi: 10.1080/17513758.2018.1484186. URL https://doi.org/10.1080/17513758.2018.1484186. PMID: 29909739.

Roberta L. DeBiasi and Meghan Delaney. Symptomatic and Asymptomatic Viral Shedding in Pediatric Patients Infected With Severe Acute Respiratory Syndrome Coronavirus 2 (SARS-CoV-2): Under the Surface. *JAMA Pediatrics*, 08 2020. ISSN 2168-6203. doi:

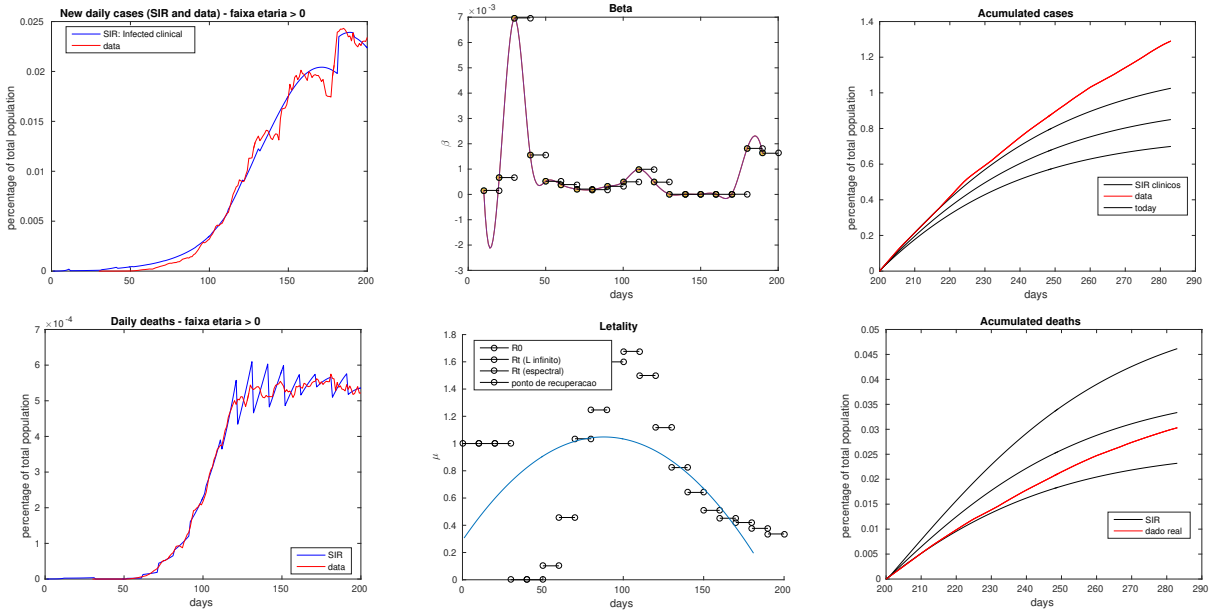

FIGURE 11. Brazil. Top left: new daily cases computed by SIR (blue) and data (red). Top middle: values of β_w. Top right: predictions for acumulated number of new cases; Bottom left: daily deaths computed by SIR (blue) and data (red). Bottom middle: μ (black) and blue curve is the least square quadratic parabola (blue). Bottom right: predictions for acumulated total deaths.

10.1001/jamapediatrics.2020.3996. URL https://doi.org/10.1001/jamapediatrics.2020.3996.

Paul L. Delamater, Erica J. Street, Timothy F. Leslie, Y. Tony Yang, and Kathryn H. Jacobsen. Complexity of the basic reproduction number (r0). *Emerging Infectious Diseases*, 25(1):1–4, 2019. doi: https://dx.doi.org/10.3201/eid2501.171901. URL https://wwwnc.cdc.gov/eid/article/25/1/17-1901_article.

John Dennis, Andrew McGovern, Sebastian Vollmer, and Bilal A Mateen. Improving covid-19 critical care mortality over time in england: A national cohort study, march to june 2020. *medRxiv*, 2020. doi: 10.1101/2020.07.30.20165134. URL https://www.medrxiv.org/content/early/2020/08/03/2020.07.30.20165134.

O. Diekmann, J. A. P. Heesterbeek, and J. A. J. Metz. On the definition and the computation of the basic reproduction ratio r_0 in models for infectious diseases in heterogeneous populations. *Journal of Mathematical Biology*, 28(4):365–382, Jun 1990. ISSN 1432-1416. doi: 10.1007/BF00178324. URL https://doi.org/10.1007/BF00178324.

Claire Donnat and Susan Holmes. Modeling the Heterogeneity in COVID-19's Reproductive Number and its Impact on Predictive Scenarios. *arXiv e-prints*, art. arXiv:2004.05272, April 2020.

Alberto d'Onofrio and Piero Manfredi. *The Interplay Between Voluntary Vaccination and Reduction of Risky Behavior: A General Behavior-Implicit SIR Model for Vaccine Preventable Infections*, pages 185–203. Springer International Publishing, Cham, 2020. ISBN 978-3-030-41120-6. doi: 10.1007/978-3-030-41120-6_10. URL https://doi.org/10.1007/978-3-030-41120-6_10.

Martin S Eichenbaum, Sergio Rebelo, and Mathias Trabandt. The macroeconomics of epidemics. Working Paper 26882, National Bureau of Economic Research, March 2020. URL http://www.nber.org/papers/w26882.

Neil M Ferguson, Daniel Laydon, and Gemma et al. Nedjati-Gilani. Impact of non-pharmaceutical interventions (npis) to reduce covid-19 mortality and healthcare demand. Technical report, Imperial College London, 03 2020.

Sebastian Funk, Shweta Bansal, Chris T. Bauch, Ken T.D. Eames, W. John Edmunds, Alison P. Galvani, and Petra Klepac. Nine challenges in incorporating the dynamics of behaviour in infectious diseases models. *Epidemics*, 10:21 – 25, 2015. ISSN 1755-4365. doi: https://doi.org/10.1016/j.epidem.2014.09.005. URL http://www.sciencedirect.com/science/article/pii/S1755436514000541. Challenges in Modelling Infectious DIsease Dynamics.

M. Gabriela M. Gomes, Rodrigo M. Corder, Jessica G. King, Kate E. Langwig, Caetano Souto-Maior, Jorge Carneiro, Guilherme Goncalves, Carlos Penha-Goncalves, Marcelo U. Ferreira, and Ricardo Aguas. Individual variation in susceptibility or exposure to sars-cov-2 lowers the herd immunity threshold. *medRxiv*, 2020. doi: 10.1101/2020.04.27.20081893. URL https://www.medrxiv.org/content/early/2020/05/21/2020.04.27.20081893.

Eduardo González and Marcelo J. Villena. On the spatial dynamics of vaccination: A spatial sirs-v model. *Computers & Mathematics with Applications*, 80(5):733 – 743, 2020. ISSN 0898-1221. doi: https://doi.org/10.1016/j.camwa.2020.04.015. URL http://www.sciencedirect.com/science/article/pii/S0898122120301620.

Veronica Guerrieri, Guido Lorenzoni, Ludwig Straub, and IvÃ¡n Werning. Macroeconomic implications of covid-19: Can negative supply shocks cause demand shortages? Working Paper 26918, National Bureau of Economic Research, April 2020. URL http://www.nber.org/papers/w26918.

W.H. Hamer. The milroy lectures on epidemic disease in england–the evidence of variability and of persistency of type. *The Lancet*, 167(4305):569 – 574, 1906. ISSN 0140-6736.

doi: https://doi.org/10.1016/S0140-6736(01)80187-2. URL http://www.sciencedirect.com/science/article/pii/S0140673601801872. Originally published as Volume 1, Issue 4305.

Mi Seon Han, Eun Hwa Choi, Sung Hee Chang, Byoung-Lo Jin, Eun Joo Lee, Baek Nam Kim, Min Kyoung Kim, Kihyun Doo, Ju-Hee Seo, Yae-Jean Kim, Yeo Jin Kim, Ji Young Park, Sun Bok Suh, Hyunju Lee, Eun Young Cho, Dong Hyun Kim, Jong Min Kim, Hye Young Kim, Su Eun Park, Joon Kee Lee, Dae Sun Jo, Seung-Man Cho, Jae Hong Choi, Kyo Jin Jo, Young June Choe, Ki Hwan Kim, and Jong-Hyun Kim. Clinical Characteristics and Viral RNA Detection in Children With Coronavirus Disease 2019 in the Republic of Korea. *JAMA Pediatrics*, 08 2020. ISSN 2168-6203. doi: 10.1001/jamapediatrics.2020.3988. URL https://doi.org/10.1001/jamapediatrics.2020.3988.

Fiona P. Havers, Carrie Reed, Travis Lim, Joel M. Montgomery, John D. Klena, Aron J. Hall, Alicia M. Fry, Deborah L. Cannon, Cheng-Feng Chiang, Aridth Gibbons, Inna Krapiunaya, Maria Morales-Betoulle, Katherine Roguski, Mohammad Ata Ur Rasheed, Brandi Freeman, Sandra Lester, Lisa Mills, Darin S. Carroll, S. Michele Owen, Jeffrey A. Johnson, Vera Semenova, Carina Blackmore, Debra Blog, Shua J. Chai, Angela Dunn, Julie Hand, Seema Jain, Scott Lindquist, Ruth Lynfield, Scott Pritchard, Theresa Sokol, Lynn Sosa, George Turabelidze, Sharon M. Watkins, John Wiesman, Randall W. Williams, Stephanie Yendell, Jarad Schiffer, and Natalie J. Thornburg. Seroprevalence of Antibodies to SARS-CoV-2 in 10 Sites in the United States, March 23-May 12, 2020. *JAMA Internal Medicine*, 07 2020. ISSN 2168-6106. doi: 10.1001/jamainternmed.2020.4130. URL https://doi.org/10.1001/jamainternmed.2020.4130.

Carl Heneghan, Jon Brassey, and Tom Jefferson. Covid-19: What proportion are asymptomatic?, 2020. URL https://www.cebm.net/covid-19/covid-19-what-proportion-are-asymptomatic/. Accessed in 29 October, 2020.

Herbert W. Hethcote. The mathematics of infectious diseases. *SIAM Review*, 42(4):599–653, 2000. ISSN 00361445. URL http://www.jstor.org/stable/2653135.

Leora Horwitz, Simon A. Jones, Robert J. Cerfolio, Fritz Francois, Joseph Greco, Bret Rudy, and Christopher M Petrilli. Trends in covid-19 risk-adjusted mortality rates in a single health system. *medRxiv*, 2020. doi: 10.1101/2020.08.11.20172775. URL https://www.medrxiv.org/content/early/2020/08/14/2020.08.11.20172775.

Mimmo Iannelli and Fabio Milner. *The basic approach to age-structured population dynamics*. Lecture Notes on Mathematical Modelling in the Life Sciences. Springer, Dordrecht, 2017. ISBN 978-94-024-1145-4; 978-94-024-1146-1. doi: 10.1007/978-94-024-1146-1. URL https://doi.org/10.1007/978-94-024-1146-1. Models, methods and numerics.

Jiwei Jia, Jian Ding, Siyu Liu, Guidong Liao, Jingzhi Li, Ben Duan, Guoqing Wang, and Ran Zhang. Modeling the control of covid-19: impact of policy interventions and meteorological factors. *Electron. J. Differential Equations*, 2020(23):1–24, 2020.

William Ogilvy Kermack, A. G. McKendrick, and Gilbert Thomas Walker. A contribution to the mathematical theory of epidemics. *Proceedings of the Royal Society of London. Series A, Containing Papers of a Mathematical and Physical Character*, 115(772):700–721, 1927. doi: 10.1098/rspa.1927.0118. URL https://royalsocietypublishing.org/doi/abs/10.1098/rspa.1927.0118.

Petra Klepac and Hal Caswell. The stage-structured epidemic: linking disease and demography with a multi-state matrix approach model. *Theoretical Ecology*, 4(3):301–319, Aug 2011. ISSN 1874-1746. doi: 10.1007/s12080-010-0079-8. URL https://doi.org/10.1007/s12080-010-0079-8.

Petra Klepac, Laura W. Pomeroy, Ottar N. Bjørnstad, Thijs Kuiken, Albert D.M.E. Osterhaus, and Jolianne M. Rijks. Stage-structured transmission of phocine distemper virus in the dutch 2002 outbreak. *Proceedings of the Royal Society B: Biological Sciences*, 276(1666):2469–2476, 2009. doi: 10.1098/rspb.2009.0175. URL https://royalsocietypublishing.org/doi/abs/10.1098/rspb.2009.0175.

Bruno Kawaoka Komatsu and Naercio Menezes-Filho. Simulando os efeitos de políticas de distanciamento Social em São Paulo usando um modelo SEIR, Maio 2020.

Michael Kremer. Integrating Behavioral Choice into Epidemiological Models of AIDS*. *The Quarterly Journal of Economics*, 111(2):549–573, 05 1996. ISSN 0033-5533. doi: 10.2307/2946687. URL https://doi.org/10.2307/2946687.

Toshikazu Kuniya and Jinliang Wang. Global dynamics of an sir epidemic model with nonlocal diffusion. *Nonlinear Analysis: Real World Applications*, 43:262 – 282, 2018. ISSN 1468-1218. doi: https://doi.org/10.1016/j.nonrwa.2018.03.001. URL http://www.sciencedirect.com/science/article/pii/S1468121818301858.

John C Lang, Hans De Sterck, Jamieson L Kaiser, and Joel C Miller. Analytic models for SIR disease spread on random spatial networks. *Journal of Complex Networks*, 6(6):948–970, 03 2018. ISSN 2051-1329. doi: 10.1093/comnet/cny004. URL https://doi.org/10.1093/comnet/cny004.

Xue-Zhi Li, Junyuan Yang, and Maia Martcheva. *Linear Age-Structured Population Models as a Base of Age-Structured Epidemic Models*, pages 1–21. Springer International Publishing, Cham, 2020. ISBN 978-3-030-42496-1.

Jose Lourenço, Robert Paton, Mahan Ghafari, Moritz Kraemer, Craig Thompson, Peter Simmonds, Paul Klenerman, and Sunetra Gupta. Fundamental principles of epidemic

spread highlight the immediate need for large-scale serological surveys to assess the stage of the sars-cov-2 epidemic. *medRxiv*, 2020. doi: 10.1101/2020.03.24.20042291. URL https://www.medrxiv.org/content/early/2020/03/26/2020.03.24.20042291.

Piero Manfredi and Alberto d'Onofrio, editors. *Modeling the interplay between human behavior and the spread of infectious diseases*. Springer, New York, 2013. ISBN 978-1-4614-5473-1; 978-1-4614-5474-8. doi: 10.1007/978-1-4614-5474-8. URL https://doi.org/10.1007/978-1-4614-5474-8.

Robert M. May and Roy M. Anderson. Spatial heterogeneity and the design of immunization programs. *Math. Biosci.*, 72(1):83–111, 1984. ISSN 0025-5564. doi: 10.1016/0025-5564(84)90063-4. URL https://doi.org/10.1016/0025-5564(84)90063-4.

A. G. M'Kendrick. Applications of mathematics to medical problems. *Proceedings of the Edinburgh Mathematical Society*, 44:98–130, 1925. doi: 10.1017/S0013091500034428.

Joël Mossong, Niel Hens, Mark Jit, Philippe Beutels, Kari Auranen, Rafael Mikolajczyk, Marco Massari, Stefania Salmaso, Gianpaolo Scalia Tomba, Jacco Wallinga, Janneke Heijne, Malgorzata Sadkowska-Todys, Magdalena Rosinska, and W. John Edmunds. Social contacts and mixing patterns relevant to the spread of infectious diseases. *PLOS Medicine*, 5(3):1–1, 03 2008. doi: 10.1371/journal.pmed.0050074. URL https://doi.org/10.1371/journal.pmed.0050074.

Seong-Hun Paeng and Jonggul Lee. Continuous and discrete sir-models with spatial distributions. *Journal of Mathematical Biology*, 74:1709–1727, 2017. doi: https://doi.org/10.1007/s00285-016-1071-8.

Pedro S. Peixoto, Diego Marcondes, Cláudia Peixoto, and Sérgio M. Oliva. Modeling future spread of infections via mobile geolocation data and population dynamics. an application to covid-19 in brazil. *PLOS ONE*, 15(7):1–23, 07 2020. doi: 10.1371/journal.pone.0235732. URL https://doi.org/10.1371/journal.pone.0235732.

T. Alex Perkins and Guido España. Optimal control of the covid-19 pandemic with non-pharmaceutical interventions. *Bulletin of Mathematical Biology*, 82(9):118, Sep 2020. ISSN 1522-9602. doi: 10.1007/s11538-020-00795-y. URL https://doi.org/10.1007/s11538-020-00795-y.

Charles Perrings, Carlos Castillo-Chavez, Gerardo Chowell, Peter Daszak, Eli P. Fenichel, David Finnoff, Richard D. Horan, A. Marm Kilpatrick, Ann P. Kinzig, Nicolai V. Kuminoff, Simon Levin, Benjamin Morin, Katherine F. Smith, and Michael Springborn. Merging economics and epidemiology to improve the prediction and management of infectious disease. *EcoHealth*, 11(4):464–475, Dec 2014. ISSN 1612-9210. doi: 10.1007/s10393-014-0963-6. URL https://pubmed.ncbi.nlm.nih.gov/25233829.

25233829[pmid].

Kiesha Prem, Alex R. Cook, and Mark Jit. Projecting social contact matrices in 152 countries using contact surveys and demographic data. *PLOS Computational Biology*, 13(9):1–21, 09 2017. doi: 10.1371/journal.pcbi.1005697. URL https://doi.org/10.1371/journal.pcbi.1005697.

Kiesha Prem, Yang Liu, Timothy W. Russell, Adam J. Kucharski, Rosalind M. Eggo, Nicholas Davies, Stefan Flasche, Samuel Clifford, Carl A. B. Pearson, James D. Munday, Sam Abbott, Hamish Gibbs, Alicia Rosello, Billy J. Quilty, Thibaut Jombart, Fiona Sun, Charlie Diamond, Amy Gimma, Kevin van Zandvoort, Sebastian Funk, Christopher I. Jarvis, W. John Edmunds, Nikos I. Bosse, Joel Hellewell, Mark Jit, and Petra Klepac. The effect of control strategies to reduce social mixing on outcomes of the covid-19 epidemic in wuhan, china: a modelling study. *The Lancet Public Health*, 5 (5):e261–e270, May 2020. ISSN 2468-2667. doi: 10.1016/S2468-2667(20)30073-6. URL https://doi.org/10.1016/S2468-2667(20)30073-6.

Weston C. Roda, Marie B. Varughese, Donglin Han, and Michael Y. Li. Why is it difficult to accurately predict the covid-19 epidemic? *Infectious Disease Modelling*, 5:271 – 281, 2020. ISSN 2468-0427. doi: https://doi.org/10.1016/j.idm.2020.03.001. URL http://www.sciencedirect.com/science/article/pii/S2468042720300075.

Moslem Soofi, Farid Najafi, and Behzad Karami-Matin. Using insights from behavioral economics to mitigate the spread of covid-19. *Applied Health Economics and Health Policy*, 18(3):345–350, Jun 2020. ISSN 1179-1896. doi: 10.1007/s40258-020-00595-4. URL https://doi.org/10.1007/s40258-020-00595-4.

Ruoyan Sun. Global stability of the endemic equilibrium of multigroup sir models with nonlinear incidence. *Computers & Mathematics with Applications*, 60(8):2286 – 2291, 2010. ISSN 0898-1221. doi: https://doi.org/10.1016/j.camwa.2010.08.020. URL http://www.sciencedirect.com/science/article/pii/S0898122110005845.

Bálint Takács and Yiannis Hadjimichael. High order discretizations for spatial dependent sir models, 2019.

S. Towers and Z. Feng. Social contact patterns and control strategies for influenza in the elderly. *Mathematical Biosciences*, 240(2):241 – 249, 2012. ISSN 0025-5564. doi: https://doi.org/10.1016/j.mbs.2012.07.007. URL http://www.sciencedirect.com/science/article/pii/S0025556412001721.

Robert Verity, Lucy C Okell, Ilaria Dorigatti, Peter Winskill, Charles Whittaker, Natsuko Imai, Gina Cuomo-Dannenburg, Hayley Thompson, Patrick Walker, Han Fu, Amy Dighe, Jamie Griffin, Anne Cori, Marc Baguelin, Sangeeta Bhatia, Adhiratha Boonyasiri,

Zulma M Cucunuba, Rich Fitzjohn, Katy A M Gaythorpe, Will Green, Arran Hamlet, Wes Hinsley, Daniel Laydon, Gemma Nedjati-Gilani, Steven Riley, Sabine van Elsand, Erik Volz, Haowei Wang, Yuanrong Wang, Xiayoue Xi, Christl Donnelly, Azra Ghani, and Neil Ferguson. Estimates of the severity of covid-19 disease. *medRxiv*, 2020. doi: 10.1101/2020.03.09.20033357. URL https://www.medrxiv.org/content/early/2020/03/13/2020.03.09.20033357.

Alex Viguerie, Guillermo Lorenzo, Ferdinando Auricchio, Davide Baroli, Thomas J. R. Hughes, Alessia Patton, Alessandro Reali, Thomas E. Yankeelov, and Alessandro Veneziani. Simulating the spread of covid-19 via spatially-resolved susceptible-exposed-infected-recovered-deceased (SEIRD) model with heterogeneous diffusion, 2020.

Patrick G. T. Walker, Charles Whittaker, Oliver J. Watson, Marc Baguelin, Peter Winskill, Arran Hamlet, Bimandra A. Djafaara, Zulma Cucunubá, Daniela Olivera Mesa, Will Green, Hayley Thompson, Shevanthi Nayagam, Kylie E. C. Ainslie, Sangeeta Bhatia, Samir Bhatt, Adhiratha Boonyasiri, Olivia Boyd, Nicholas F. Brazeau, Lorenzo Cattarino, Gina Cuomo-Dannenburg, Amy Dighe, Christl A. Donnelly, Ilaria Dorigatti, Sabine L. van Elsland, Rich FitzJohn, Han Fu, Katy A. M. Gaythorpe, Lily Geidelberg, Nicholas Grassly, David Haw, Sarah Hayes, Wes Hinsley, Natsuko Imai, David Jorgensen, Edward Knock, Daniel Laydon, Swapnil Mishra, Gemma Nedjati-Gilani, Lucy C. Okell, H. Juliette Unwin, Robert Verity, Michaela Vollmer, Caroline E. Walters, Haowei Wang, Yuanrong Wang, Xiaoyue Xi, David G. Lalloo, Neil M. Ferguson, and Azra C. Ghani. The impact of covid-19 and strategies for mitigation and suppression in low- and middle-income countries. *Science*, 369(6502):413–422, 2020. ISSN 0036-8075. doi: 10.1126/science.abc0035. URL https://science.sciencemag.org/content/369/6502/413.

Xiaowei Wen, Juping Ji, and Bo Li. Asymptotic profiles of the endemic equilibrium to a diffusive sis epidemic model with mass action infection mechanism. *Journal of Mathematical Analysis and Applications*, 458(1):715 – 729, 2018. ISSN 0022-247X. doi: https://doi.org/10.1016/j.jmaa.2017.08.016. URL http://www.sciencedirect.com/science/article/pii/S0022247X17307734.

Yixiang Wu and Xingfu Zou. Asymptotic profiles of steady states for a diffusive sis epidemic model with mass action infection mechanism. *Journal of Differential Equations*, 261(8): 4424 – 4447, 2016. ISSN 0022-0396. doi: https://doi.org/10.1016/j.jde.2016.06.028. URL http://www.sciencedirect.com/science/article/pii/S0022039616301644.